A continuous model for sand dunes and its application to barchan dunes

O. Durán
Multi Scale Mechanics (MSM), Twente University, Netherlands

E.J.R. Parteli
Departamento de Física, Universidade Federal do Ceará, Brazil

H.J. Herrmann
Computational Physics, ETH, Zürich, Switzerland

ABSTRACT: In this work we present an updated version of an existing continuous dune model which contains important modifications to improve its predicting power. Further, we use the model to simulate isolated barchan dunes and extract the relations describing their morphology and dynamics. Finally, we study their stability and show that they are intrinsic unstable bed-forms.

1 INTRODUCTION

The existence of a minimal size for aeolian dunes of about 10 − 20 m wide has been the main reason behind the many attempts for the numerical simulation of such bed-forms (Werner 1995, Andreotti 2002ab, Kroy 2002). In particular, the continuous 'minimal' model developed by Sauerman et al. (2001) has been successfully extended to include 3D transversal and barchan dunes (Schwämmle 2005), dunes collisions (Schwämmle 2003), vegetation and parabolic dunes (Duran 2006b), Martian dunes (Parteli 2007a) and very recently, linear dunes (Parteli 2007b) and barchan dune fields (Duran 2007) (Fig. 1).

Since the previous work in the modelling of barchan dunes (Sauermann 2001b, Kroy 2002, Schwäammle 2005), the 'minimal' dune model has experienced several changes, both in the wind model (Duran 2005), where now we use the non-asymptotic solution for the shear stress perturbation over a smooth hill (Weng 1991), and a modify sand transport model (Duran 2006a). Although small, these changes affect the dune morphology and lead to important consequences in the modelling of dune fields (Duran 2007).

In this work we present our current version of such 'minimal' model along with simulations of aeolian barchan dunes (Fig. 2). In order to validate the model, we compare the morphology of simulated barchans with measured ones in Morocco (Sauermann 2000). Furthermore, we derive relations for the volume, velocity and outflux of barchan dunes, that are consistent with recent measurements (Elbelrhiti 2007). Finally, we apply such relations to study the stability of an isolated barchan dune.

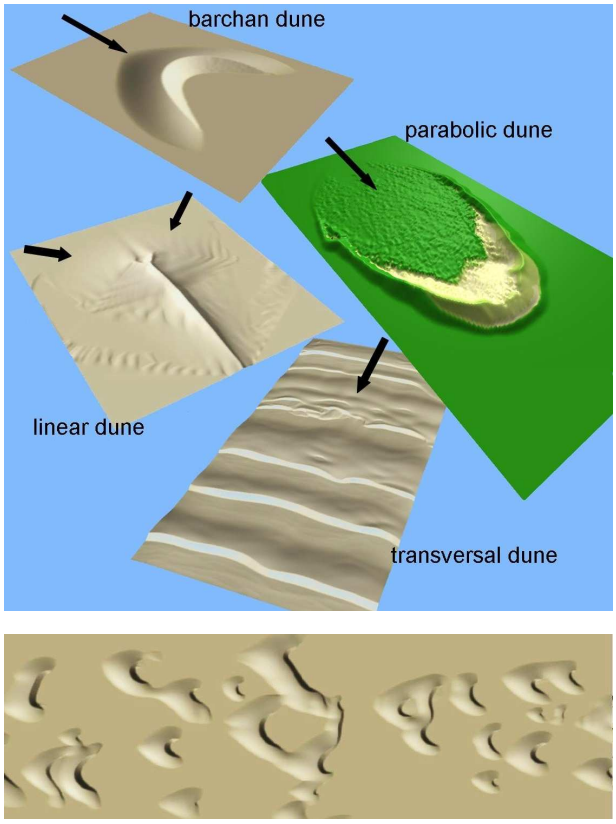

Figure 1. Top: different types of aeolian dunes simulated with the current 'minimal' model. Arrows indicate wind direction. Bottom: a first attempt to simulate a barchan dune field.

2 DUNE MODEL

The modelling of dunes involves three main stages: (i) a calculation of the wind considering the influence of the topography, (ii) a calculation of the sand flux carry by the perturbed wind, and finally (iii) the evolution of the sand surface due to sand erosion, deposition and avalanches. Once the wind starts to blow, it is deformed by the surface topography experiencing a speedup on positives slopes and a slowdown on negatives ones. This spatial perturbation of the wind velocity leads to an inhomogeneous sand flux. Therefore, the sand surface changes due to the erosion and deposition processes, which are determined by the change of the sand flux in the transport direction. This topographic change in turn induces a new perturbation on the wind field and the whole cycle repeats again.

The coupling sand surface evolution and aeolian sand transport involves two different time scales related, on one hand, to erosion and deposition processes that change the surface, and, on the other hand, to sand transport and wind flow. A significant change in sand surface can happen within some hours or even days. In contrast, the time scale of wind flow changes and saltation process is much faster, of the order of seconds. This separation of time scales leads to an enormous simplification because it decouples the different processes. Therefore, we can use stationary solutions for the wind surface shear velocity u_* and for the resulting sand flux $\mathbf{q}$, and later use them for the time evolution of the sand surface $h(x, y)$.

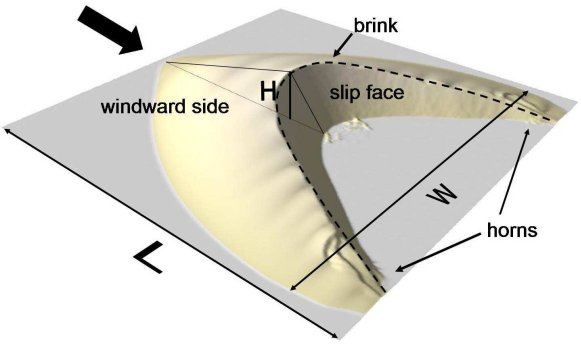

Figure 2. Barchan dune.

2.1 *Wind model*

The sand transport rate is determined not by wind velocity, which change with height, but rather by the shear velocity which encodes the friction forces at the surface. The surface shear velocity not only changes with the sediment transport via the feedback effect, but also with the terrain topography. It is well known that a uphill induces a wind speedup while a downhill produces a wind slowdown. This change in the wind velocity is crucial for the understanding of dune formation and migration.

We consider a low and smooth topographic accident $h_s(x, y)$, like a hill or a sand dune, which induces a small perturbation $\delta\mathbf{v}(x,y,z)$ in the wind velocity profile, namely

$$\vec{v}(x,y,z) = \vec{v}_0(z) + \delta\vec{v}(x,y,z) \quad (1)$$

where $\mathbf{v}_0(z)$ is the unperturbed wind velocity profile.

From the Prandlt turbulent closure, a velocity perturbation leads to a modification of the surface shear stress $\boldsymbol{\tau}_0$ over a flat bed given by:

$$\vec{\tau}(x,y) = \vec{\tau}_0 + |\vec{\tau}_0|\delta\vec{\tau}(x,y) \quad (2)$$

where $\delta\boldsymbol{\tau}(x, y)$ is the shear stress perturbation at the surface $h_s(x, y)$. From now on subscript '0' means values on a flat bed.

The shear stress perturbation $\delta\boldsymbol{\tau}$ is computed according to an analytical work describing the influence of a low and smooth hill in the wind profile and shear stress (Weng 1991). In the Fourier space, this perturbation is proportional to the Fourier transform of the height profile h_s, and depends on the apparent roughness length of the surface, which could takes into account saltation (Duran 2006a) and on the typical length scale L of the hill. This length is defined as the mean wavelength of the Fourier representation of the height profile.

By inserting the inverse Fourier-transform of the perturbation into Eq. (2) one obtains the modified shear stress, which in terms of the shear velocity reads:

$$\vec{u}_*(x,y) = u_*(x,y)\vec{e}_\tau(x,y) \quad (3)$$

where the unity vector $\mathbf{e}_\tau \equiv \boldsymbol{\tau}/|\boldsymbol{\tau}|$ defines the actual wind direction and the perturbed shear velocity is:

$$u_*(x,y) \approx u_{*0}\sqrt{1+\delta\tau_x(x,y)} \quad (4)$$

Here $u_{*0}=(\tau_0/\rho)^{1/2}$ denotes the unperturbed shear velocity in a flat bed.

2.1.1 *Separation bubble*

The formalism for computing the surface wind perturbation does not include nonlinear effects like flow separation and, therefore, it is only valid for smooth surfaces. However, in sand dunes the brink line not only divides the face where avalanches occurs from the rest of the dune, but also, since the repose angle of sand (~34°) represents the highest slope in the dune surface, it establishes a limit at which the wind streamlines separate from the surface (Fig. 2). Therefore the above model cannot be used for mature sand dunes with slip faces. One solution for this problem (Sauermann 2001b), is to calculate the wind pertur-

bation over an ideal smooth surface $h_s(x, y)$ that comprise the profile $h(x, y)$ of the dune and the so called separation bubble $s(x, y)$.

The separation bubble is defined as the surface that limits the region of recirculating flow after the brink that results from flow separation (Fig. 3). In this region the flow is strongly depressed and thus sand transport can be neglected in first approximation. Following the Sauermann (2001) approach, each slice of the surface of the bubble should resembles the separating streamline shape and is modeled by a third-order polynomial so that, in the case of a barchan, the region between the horns is inside the bubble (Fig. 4ab). The coefficients of this polynomial arise from the continuity of both surfaces at the brink line $x_b(y)$, where $x_b(y)$ is the x-position of the brink for each slice y (Fig. 3), the continuity of the first derivatives at the brink, and the smooth conditions $h_s(x_r(y))=0$ and $h_s'(x_r(y))=0$ at the reattachment line $x_r(y)$, where flow re-attach to the surface again. The reattachment length $l(y) \equiv x_r(y)- x_b(y)$ for each slice y (Fig. 3), is obtained from the assumption that the separation surface has a maximum slope.

Figure 4ab show a simulated barchan dune without and with the separation bubble, respectively. The resultant surface $h_s(x, y \equiv \max(h(x, y), s(x, y))$ is then used to calculate the wind shear velocity perturbation on a barchan dune according to Eqs. (3), as depicted in Figure 4c. The dune topography induces two kinds of variations on the wind shear. First a variation in the strength: at the dune's foot, wind experiences a slowdown, followed by a speedup at the windward side and later again a slowdown at dune's horns (see the x-component of the wind, Figure 4d). And, second, a variation in wind direction since the wind is forced to surround the dune, as shows Figure 4e.

Finally, based on the flow separation at the brink, we set the shear velocity to zero below the separation bubble, i.e. $u_*(x,y)=0$ for $h(x, y) < h_s(x, y)$.

The corresponding new shear velocity $\mathbf{u}_*(x,y)$ is used afterwards to calculate the sand transport on the surface $h(x, y)$.

2.2 *Three dimensional sand transport model*

2.2.1 *Characteristic velocity of sand grains*

From the shear velocity, the modification of the air flow due to the presence of saltating grains is accounted for. Within the saltation layer the feedback effect of sand transport results in an effective wind velocity driving the grains (Duran 2006a). This effective wind velocity v_{eff} is given by the wind velocity $v(x, y, z_1)$ at a reference height z_1. By assuming as a first approximation no focal point (Duran 2006a), and taking into account the range of the characteristic height of the saltation layer z_m ~ 20 mm, the grain based roughness length z_0 ~10 μm and the reference height z_1 ~ 3 mm, the effective wind velocity can be approximated as (Duran 2006a):

$$v_{eff}(x,y) \approx \frac{u_{*t}}{\kappa}\left[\ln\frac{z_1}{z_0} + \frac{z_1}{z_m}\left(\frac{u_*(x,y)}{u_{*t}} - 1\right)\right] \qquad (5)$$

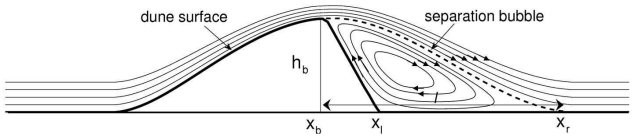

Figure 3. Sketch of the central slice of a barchan dune with the separation bubble. In the ideal case the flow separation generates a rotational flow in the region inside the bubble with a negligible sand transport.

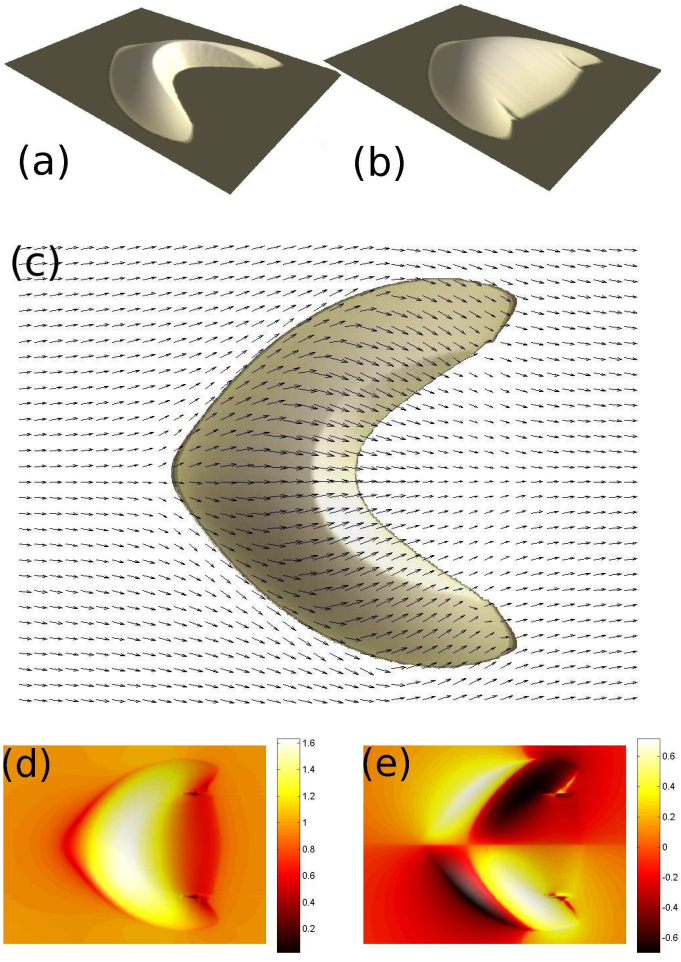

Figure 4: Simulated barchan dune (a) and its separation bubble (b). The normalized wind shear velocity $\mathbf{u}_*/ u_{*0}$ (Eq. 3) over a barchan dune including the separation bubble (b), is plotted in (c). Note that u_ is proportional to the wind velocity field at a fixed height. Both component u_{*x} and u_{*y} are included in (d) and (e) for comparison.

where u_{*t} is the shear velocity threshold for sand transport.

The collective motion of sand grains in the saltation layer is characterized by their horizontal velocity us at the reference height z_1, which for simplicity is called sand grain velocity although it is referred to the total grain horizontal motion and not to individual grains. In the saturated state this velocity is determined from the momentum balance between the drag force acting on the grains, the loss of momentum when they splash on the ground, and the downhill gravity force (Sauermann 2001a, Kroy 2002)

$$\frac{\left(\vec{v}_{eff}-\vec{u}_s\right)\left|\vec{v}_{eff}-\vec{u}_s\right|}{u_f^2}-\frac{\vec{u}_s}{2\alpha\left|\vec{u}_s\right|}-\nabla h=0 \qquad (6)$$

where $\mathbf{v}_{\text{eff}} \equiv v_{eff}\,\mathbf{e}_\tau$ and u_f is the grain settling velocity.

For step surfaces Eq. (6) must be solve numerically. However, since dunes has not slopes exceeding the repose angle of sand (~34°), the sand transport direction $\mathbf{u}_s/|\mathbf{u}_s|$ in the friction term can be approximated by the wind direction $\mathbf{e}_\tau$. In this case the sand grains velocity is given by:

$$\vec{u}_s \approx \left(v_{eff}-\frac{u_f}{\sqrt{2\alpha}A}\right)\vec{e}_\tau-\frac{\sqrt{2\alpha}u_f}{A}\nabla h \qquad (7)$$

where $A \equiv |\mathbf{e}_\tau + 2\alpha \text{ grad } h|$. From this equation, the sand velocity in the saturated state has two terms. The first one points toward the wind direction, while the second one is directed along the surface gradient. Both terms account for the competing effects of wind blown and gravity on the motion of sand grains. Figure 5 shows the characteristic horizontal velocity of sand grains over a barchan dune. Note the strong deviation of the sand flux at the dune's base and the 'trap' effect of the slip face due to flow separation at the brink. The trapped grains accumulate on the top of the slip face before falling down in avalanches.

2.2.2 *Saltation flux*

From Eq. (6) we can obtain the saturated sand flux q_s over an irregular sand surface $h(x, y)$. However, how the sand flux reach the saturated state from a given initial or boundary value?

From the first section we know that in one hand the saltation sand flux over a sand bed can increase due to the cascade of splashed grains that enter to the flow, while in the other hand, it cannot unlimited grow due to the feedback effect of the grain motion on the wind shear. Therefore, Sauermann et al. proposed a transport equation that describes the spatial evolution of the saltation sand flux $q \equiv |\mathbf{q}|$ (Sauermann 2001a):

$$\nabla\cdot\vec{q}=\frac{q}{l_s}\left(1-\frac{q}{q_s}\right)\left[\Theta(h)\Theta(q_s-q)+\Theta(q-q_s)\right] \qquad (8)$$

where $q_s \equiv |\mathbf{q}_s|$ is the saturated sand flux and l_s is the characteristic length for saturation and thus is called 'saturation length'. From Eq. (8) the spatial change of sand flux for small values of q is driven by the exponential growth term q/l_s, with the characteristic length l_s, while for values of q close to the maximum q_s, the second term $1 - q/q_s$ leads to a saturated state. Symbol $\Theta(x)$ represents the Heaviside function, and guarantees that if there is no sand available ($h = 0$) an undersaturated sand flux $q < q_s$ cannot increase.

Both, the saturated sand flux and the saturation length are given by:

$$\vec{q}_s(u_*)=\frac{2\alpha}{g}\frac{\rho}{\rho_{sand}}\left(u_*^2-u_{*t}^2\right)\vec{u}_s \qquad (9)$$

$$l_s(u_*)=\frac{2\alpha\left|\vec{u}_s\right|^2}{\gamma g}\frac{1}{\left(u_*/u_{*t}\right)^2-1} \qquad (10)$$

where α is the effective restitution coefficient (Duran 2006a) and γ is a model parameter accounting for the splash process (Sauermann 2001b). From now on we denote the saturated flux over a flat bed as $Q \equiv q_s(u_{*0})$.

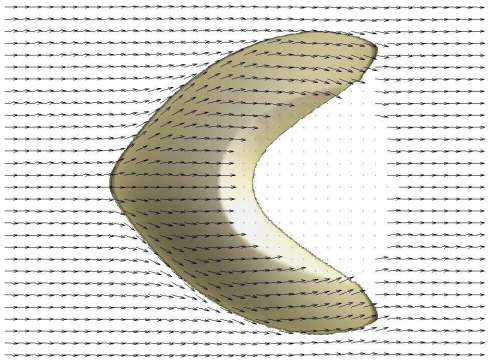

Figure 5. Vector diagram of the normalized characteristic sand grains velocity $\mathbf{u}_s/u_{s0}$ over a barchan dune. The normalization constant is defined as $u_{s0} \equiv u_s(u_{*0})$ and represents the sand velocity on a flat bed.

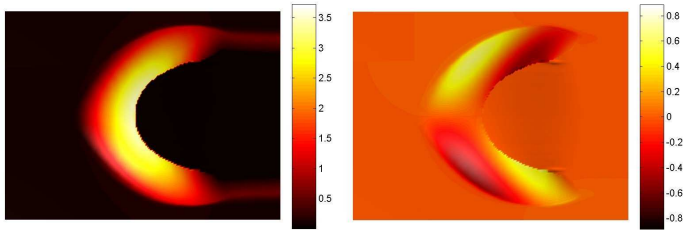

Figure 6. *X*-component (along the wind direction, left) and *y*-component (right) of the normalized saltation sand flux q/Q over a barchan dune. The flux is calculated from the wind field depicted in Figure 4. Wind blown from left to right carrying a normalized influx equal to 0.1. Although the *x*-component of

the flux is clearly higher than the transverse component, this is not negligible.

Figure 6 depicts the normalized saltation sand flux q/Q over a barchan dune that results from solving Eq.(8) with an imposed boundary condition. In this case we impose a small influx $q_{in} = 0.1\ Q$. In the figure, the barchan dune is surrounded by a flat rocky surface. Therefore, the sand flux remains constant until it reaches the sand surface. Afterwards, flux increases following the trend of the wind shear velocity (Fig. 4) i.e. the flux increases in the windward side of the dune and decreases in the dune's horns, while in the region covered by the separation bubble (the slip face and between the horns) there is no sand motion and thus no sand flux.

2.3 *The time evolution of the surface*

The spatial change of the sand flux showed in Figure 6 and described by the logistic sand transport Eq. (8) defines the change of the sand profile $h(x, y)$. According to the mass conservation:

$$\frac{\partial h}{\partial t} = -\nabla \cdot \vec{q} \qquad (11)$$

Following Eq. (8), wherever sand flux is undersaturated ($q < q_s$) the amount of sand transported by the wind can increase and erosion takes place ($\partial h/\partial t > 0$). Otherwise, in case of oversaturation ($q > q_s$), the amount of sand wind carries is beyond its limits and deposition occurs ($\partial h/\partial t < 0$).

Figure 7 shows the sand erosion-deposition pattern over a barchan dune. The dune is clearly divided into two parts, the windward side where erosion takes place and the dune's lee side, comprising the slip face and the horns, where sand is deposited. Furthermore, through erosion-deposition process given by Eq. (11) the dunes are by definition not static but dynamics objects. They are essentially sculpted by the wind, which takes sand from one place to other following certain rules. This explains how a millimetre scaled process like sand transport by saltation can produce large structures like dunes. It is not the transport mechanisms but the wind field and its interdependence with the surface morphology, what lies behind the dunes formation and evolution.

2.4 *Avalanches*

The evolution of a sand surface is determined, as was previously shown, by the aeolian erosion-deposition process, as a consequence of the inhomogeneity of the sand flux over the surface. However, in the slip face below the separation bubble there is no sand transport, therefore, sand grains accumulate there, after crossing the brink. In this region a non-aeolian mechanism of sand transport takes place, namely, sand avalanches.

Taking into account that the characteristic time of avalanches events is orders of magnitude smaller than the characteristic time involved in the whole surface evolution, we consider an effective model that instantaneously relax the gradient of the sand surface toward the sand repose angle. If the slope of the sand surface exceeds the static angle of repose, sand is redistributed according to the sand flux:

$$\vec{q}_{aval} = E\left(\tanh|\nabla h| - \tanh\left(\tan\theta_{dyn}\right)\right)\frac{\nabla h}{|\nabla h|} \qquad (12)$$

Afterwards, using this flux, the surface is repeatedly changed according to Eq. (11), until the maximum slope lies below the dynamic angle of repose, θ_{dyn}. We include the hyperbolic tangent function to improve convergence.

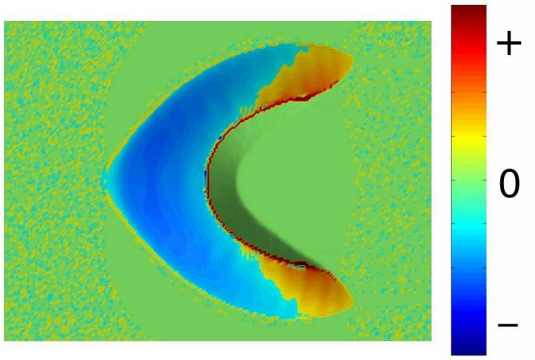

Figure 7. Sand erosion (+) and deposition (-) pattern on a barchan dune. Note that sand is eroded from the dune's windward side while it is trapped by the slip face or deposited on the horns.

2.5 *Model parameters*

2.5.1 *Wind model*

The wind model has only two parameters, the apparent roughness length and the shear velocity u_{*0} over a flat bed. The first one is fixed to the value 1 mm, which coincides with the peak value of the roughness length curve in (Duran 2006a) for the characteristic grain diameter in sand dunes $d \approx 0.25$ mm. The unperturbed shear velocity u_{*0} is defined by the initial condition.

2.5.2 *Separation bubble model*

The model for the separation bubble only has one parameter, the maximum slope allowed for the separation surface, which is fixed to the value 0.2, smaller than the value assigned by Sauermann (0.25) corresponding to an maximum angle of 14° (Sauermann 2001b). We selected 0.2 after performing calculations of wind profiles over real Moroccan dunes.

2.5.3 *Sand transport model*

The sand transport model has five parameters. Four of them, z_0, z_m, z_1 and α, are given in Duran (2006a) in terms of the grain density $\rho_g \approx 2650$ kg/m^3, grain diameter $d \approx 0.25$ mm, air density $\rho \approx 1.225$ kg/ m^3, air kinematic viscosity $\nu \approx 1.5\ 10^{-5}$ m^2/s, gravity acceleration $g \approx 9.8$ m/s^2 and drag coefficient C_d, and thus they are not free parameters. The last one is $\gamma = 0.2$ (Sauermann 2001a).

2.5.4 *Avalanches model*

The only free parameter in the model for avalanches is E which has dimension of flux. After some test of convergence we select the value $E = 0.9$ kg/ms. Of course, since the avalanches are modelled just as a slope relaxation, the value of E has no physical meaning. The other two parameters are the static $\theta_{stat} \approx 34°$ and dynamic angle of repose $\theta_{dyn} \approx 33°$ for sand.

3 BARCHAN DUNE SIMULATIONS

In this section we study barchan dunes through numerical simulations and present some scaling relations between the barchan volume, velocity and flux balance with their size. Comparing these scaling laws with measured data we validate the predictions of our dune model including a new sand transport model and the corresponding parameters (Duran 2006a).

Barchans are isolated sand dunes that emerge when wind is uni-directional and sand is sparse (see Fig. 2). Under these conditions the barchan shape represents the equilibrium shape toward which any initial sand surface over a non-erodible substrate evolves. They arise from the numerically integration of the equations (3), (8) and (11) for a given initial surface, an unperturbed shear velocity u_{*0}, oriented along the x-direction, and a constant influx q_{in} at the input boundary $x = 0$. Since u_{*0} unequivocally defines the maximum sand flux Q over a flat bed, we can use either u_{*0} or Q to characterize the unperturbed wind.

Therefore, the simulations only have two free parameters, the sand supply, encoded in q_{in}, and the wind strength, encoded in u_{*0} or $Q(u_{*0})$.

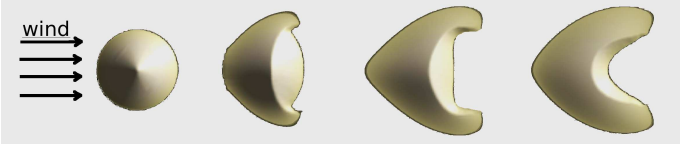

Figure 8. Formation of a 6 m high barchan dune from an initial sand pile after ~ 1 year of constant wind blow.

Figure 8 depicts the evolution of the profile $h(x, y)$ of a sand pile towards a barchan dune, while Figure 9 compares the 3-dimensional characteristic 'C' shape of a simulated and a measured Moroccan barchan (Sauermann 2000). Both dunes are very similar except at the horns. This typical simulation was performed using zero influx $q_{in} = 0$ and a flat bed shear velocity $u_{*0} = 0.4$ m/s, a realistic value for dune fields.

3.1 *Morphologic relationships*

The morphology of a barchan dune is characterized by well known linear scalings between the dune's width W, total length L, windward side length L_w, mean horns length L_h and the dune's height H (Hastenrath 67, Lettau 69, Sauermann 2000).

Figure 10 shows one of these scalings, the width-height relationship, which has the form $w = a_w H + b_w$. Therefore, the barchan shape is only scale invariant for large sizes, i.e. the ratio $H/w = H/(a_w H + b_w)$ tends to the constant $1/a_w$ at large H. However, for small sizes, $H < 5b_w/a_w \sim 2$ m, the barchan shape is size dependent. This rupture of the scale invariance at small sizes is consequence of the saturation length l_s defined in Eq. (10) (Kroy 2002, Andreotti 2002a). The saturation length also determines the minimal size for barchan dunes.

Simulations for different wind strength and influx show that the barchan volume V scales as w^3 with a proportionality factor c that is independent of both, the sand flux over a flat bed Q and the influx q_{in} (Sauermann 2001b). The value $c = 0.018$ is obtained from the fit in (Fig. 10). This simple scaling was also recently found in field measurements (Hersen 2004, Elbelrhiti 2007).

3.2 *Velocity*

Since the pioneer work of Bagnold (1941) it is also well known that the barchan velocity v scales with the inverse of its size and is proportional to the saturated flux Q on a flat bed. However, although the relationship between v and Q is well established, there is still a debate about which size one should use. Bagnold showed, through a simple mass conservation analysis, that v should scale with the inverse of the dune's height. Alternatively, other authors propose a scaling with the dune's length (Sauermann 2001b, Schwämmle 2005), or a more complex relation of the type $1/(H + H_0)$ to fit dune measurements (Andreotti 2002ab, Hersen 2004, Elbelrhiti 2007).

Using simulated barchans we find that the velocity v scales with the inverse of their width w, as shown in Figure 11. Therefore, we consider:

$$v \approx \alpha Q / w \qquad (13)$$

with the constant $\alpha \approx 50$ in very good agreement with previous studies (Hersen 2005). Taking into account the morphological relationship of a barchan, both, its length L and width w scale with the height H as $a(H + H_0)$, where the constants a and H_0 are different in both cases. Therefore, in a certain way all these scaling for the velocity are equivalent.

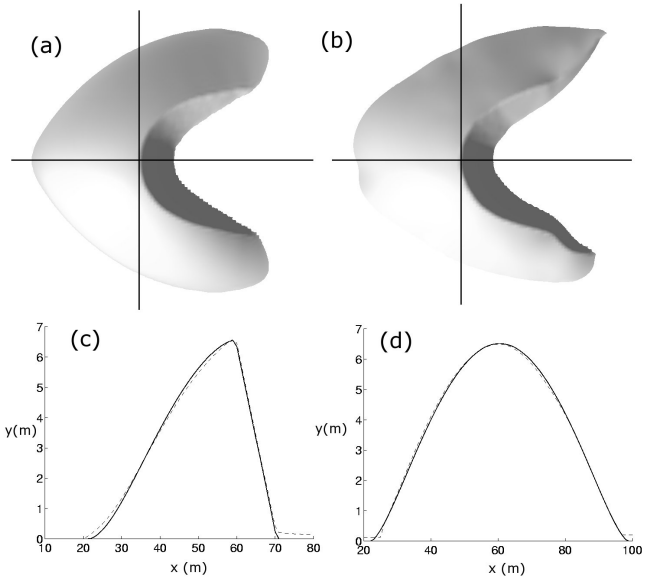

Figure 9: Comparison between a 6 m high simulated barchan (a) and a measured one (b). In (c) and (d) are shown the longitudinal (c) and transversal (d) central slides of both, the simulated and the measured dune. Dashed-line slices correspond to a measured barchan, whereas the full lines to a simulated one. Both dunes have the same scale.

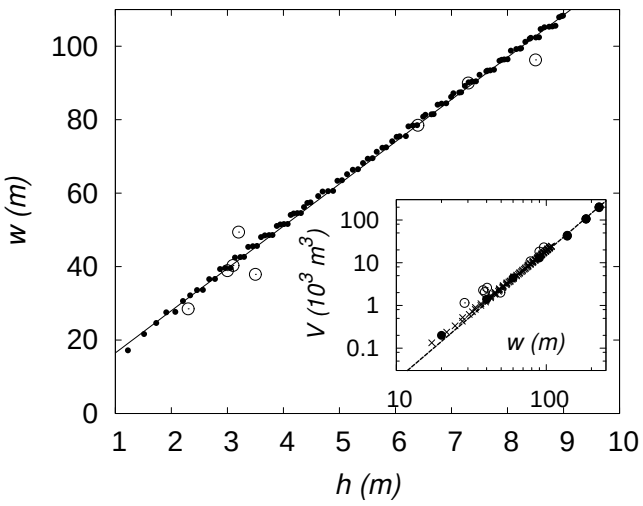

Figure 10: Height h and width w relationship for dunes in Morocco measured by Sauermann (2000) (open circles) and for simulated ones (full circles) with the linear regression $w = 12h + 5$m. Inset: Cubic scaling of the volume of simulated barchan dunes with their width. The volume data of measured Moroccan dunes (open circles) is included for comparison.

3.3 *Stability: Flux balance in a barchan dune*

From the dynamical point of view the stability of barchan dunes is a particular important question. Based on previous simulations it has been predicted that barchan dunes are intrinsically unstable (Sauermann 2001b, Hersen 2004).

In order to illustrate the dune size instability we analyze the flux balance equation. A barchan dune can be seen as an object that captures some amount of sand from the windward side and releases another amount from the horns while trapping a fraction at the slip face (Fig. 6). Therefore, the flux balance in a dune is given by the difference between the net influx Q_{in} and the net outflux Q_{out}. Since both scale with the product w Q, the volume conservation reads:

$$\frac{dV}{dt} = Q_{in} - Q_{out} = wQ\left(\frac{q_{in}}{Q} - \frac{q_{out}}{Q}\right) \qquad (14)$$

where q_{in} and q_{out} are the dune influx and outflux per unit length, respectively, and V is the volume of the dune.

Measurements on single simulated barchans with a constant influx show that for small widths $w < w_c$ the outflux is saturated which means that the dune lacks of slip-face, i.e. it becomes a dome. For higher width however, the outflux relax as $1/w^2$ to a constant value that scales linearly with the influx with a slope smaller that one (Fig. 12), namely

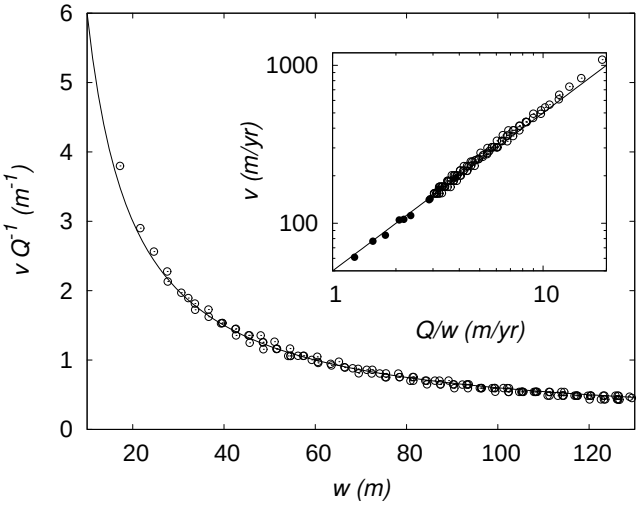

Figure 11. The velocity of simulated barchan dunes (symbols) scales as $1/w$ (full line) for a constant saturated flux Q. Inset: barchan dune velocity as a function of the ratio Q/w for different values of Q.

Figure 12. Relation between the dune outflux and the dune width w. The solid line represents the scaling with $1/w^2$ given in the text. Inset: the dune outflux is a linear function of the dune influx (solid line) with a slope smaller that one (dashed line).

$$\frac{q_{out}}{Q} = a\frac{q_{in}}{Q} + b + \left(\frac{w_c}{w}\right)^2 \qquad (15)$$

where $a \approx 0.45$, $b \approx 0.1$ and w_c are fit parameters. Therefore, there are two different regimes, for $q_{in} < 0.18Q$ the outflux is higher that the influx and the dune shrinks, while for $q_{in} > 0.18Q$ the influx overcomes the outflux and the dune grows (Fig. 12). The dimensionless barchan outflux q_{out}/Q is proportional to the total horns width fraction $2w_h/w$, where w_h denotes the width of one horn (Fig. 2). Thus, the flux balance on a barchan dune is determined by its morphology.

The deviation from the scale invariance in the dune outflux q_{out} is expressed by the last term of Eq. (15), which is a consequence of the non-scale invariance of small dunes. However, since the critical width $w_c \sim 10$m is of the order of the minimal dune width, the nonlinear term is very small and can be neglected. Therefore, we can consider in first approximation dune horns as scale invariant, in agreement with measurements on barchan dunes in south Morocco and in the Arequipa region, Peru (Elbelrhiti 2007).

In this case, combining Eqs. (14), (15) and the volume scaling $V = c\,w^3$, the mass balance becomes"

$$\frac{dw}{dt} = \frac{(1-a)Q}{3cw}\left(\frac{q_{in}}{Q} - \frac{q_c}{Q}\right) \qquad (16)$$

where $q_c = bQ/(1 - a) \approx 0.18Q$ denotes the equilibrium influx at which the dune volume does not change. However, this equilibrium is unstable since there is no mechanisms by which barchan dunes can adjust the outflux to a given influx.

4 CONCLUSIONS

We have presented the current version of the 'minimal' dune model, which has been the core of several bed-forms simulations, ranging from parabolic (Duran 2006b) to linear dunes (Parteli 2007b) (Fig. 1). The model was qualitatively validated by comparing some characteristic parameters of simulated barchan dunes with empirical data provided (Sauermann 2000, Elbelrhiti 2007). Finally, we studied the stability of barchan dunes showing that they are intrinsically unstable, a result that is in deep contradiction with the widespread existence of barchan dunes all around the world (Hersen 2004, Elbelrhiti 2007).

Furthermore, the detailed study of the behaviour of isolated barchan dunes could help to model them as single objects to be further used as the main elements of a simplified model for the dynamics of a barchan dune field (Duran 2007).

Although this continuous dune model correctly describes the main aspects of the barchan morphology and dynamics, we want to stress that it is far from being perfect. For instance, the separation bubble neglects the secondary sediment transport in the slip face and between the horns; the saturation length does not includes the inertia of sand grains and thus it fails at large winds; and the well established dependence of the shear stress threshold with the local slope is neglected (Andreotti 2007, Parteli 2007c).

5 REFERENCES

Andreotti, B., Claudin, P. & Douady, S. 2002a. Selection of dune shapes and velocities part 1: Dynamics of sand, wind and barchans. *Eur. Phys. J. B* 28:321–339.

Andreotti, B., Claudin, P. & Douady, S. 2002b. Selection of dune shapes and velocities; part 2: A two-dimensional modelling. *Eur. Phys. J. B* 28:315–319.

Andreotti, B. & Claudin, P. 2007. Comment on "Minimal size of a barchan dune". *to appear in Phys. Rev. E.*

Bagnold, R. A. 1941. The physics of blown sand and desert dunes. Methuen, London.

Durán, O., Schwämmle, V. & Herrmann, H.J. 2005. Breeding and solitary wave behavior of dunes. *Phys. Rev. E* 72:021308.

Durán, O. & Herrmann, H.J. 2006a. Modelling of saturated sand flux. *J. Stat. Mech.* P07011.

Durán, O. & Herrmann, H.J. 2006b. Vegetation against dune mobility.
Phys. Rev. Lett. 97:188001.

Durán, O. 2007. Vegetated dunes and barchan dune fields. PhD thesis, University of Stuttgart.

Elbelrhiti, H., Andreotti, B. & P. Claudin. 2007. Barchan dune corridors: field characterization and investigation of control parameters. *To appear in J. Geo. Res.* cond-mat/0609120.

Hastenrath, S. 1967. The barchans of the Arequipa region, southerPeru. *Zeitschrift für Geomorphologie* 11:300–331.

Hersen, P., Andersen, K.H., Elbelrhiti, H., Andreotti, B., Claudin, P. & Douady, S. 2004. Corridors of barchan dunes: stability and size selection. *Phys. Rev. E* 69:011304.

Hersen, P. 2005. Flow effects on the morphology and dynamics of aeolian and subaqueous barchan dunes. *J. Geophys. Res*. 110:F04S07.

Kroy, K., Sauermann, G. & Herrmann, H.J. 2002. Minimal model for sand dunes. *Phys. Rev. L*. 68:54301.

Lettau, K. & Lettau, H. 1969. Bulk transport of sand by the barchans of the Pampa de La Joya in southern Peru. *Zeitschrift für Geomorphologie* N.F.13-2:182–195.

Parteli, E.J.R. & Herrmann,H.J. 2007a. Saltation transport on Mars. *Phys. Rev. Lett.* 98:198001.

Parteli, E.J.R. 2007b. Sand dunes on Mars and on Earth. PhD thesis, University of Stuttgart.

Parteli, E.J.R., Durán, O. & Herrmann,H.J. 2007c. Reply to "Comment on "Minimal size of a barchan dune". *to appear in Phys. Rev. E*.

Sauermann, G., Rognon, P., Poliakov, A. & Herrmann, H.J. 2000. The shape of the barchan dunes of southern Morocco. *Geomorphology* 36:47–62.

Sauermann, G., Kroy, K. & Herrmann, H.J. 2001a. A continuum saltation model for sand dunes. *Phys. Rev. E* 64:31305.

Sauermann, G. 2001b. Modeling of wind blown sand and desert dunes. PhD thesis, University of Stuttgart.

Schwämmle, V. & Herrmann, H.J. 2003. Solitary wave behaviour ofdunes. *Nature* 426:619.

Schwämmle, V. & Herrmann, H.J. 2005. A model of barchan dunes including lateral shear stress. *Eur. Phys. J. E* 16:57–65.

Weng, W.S., Hunt, J.C.R., Carruthers, D.J., Warren, A., Wiggs, G.F.S., Livingstone, I. & Castro, I. 1991. Air flow and sand transport over sand–dunes. *Acta Mechanica (Suppl.)* 2:1–22.

Werner, B.T. 1995. Eolian dunes: computer simulations and attractor interpretations. *Geology* 23: 1107-1110.